

Diffusional Barrier in the Unfolding of a Small Protein

Lovy Pradeep and Jayant B. Udgaonkar*

National Centre for Biological
Sciences, Tata Institute of
Fundamental Research
GKVK Campus
Bangalore 560 065, India

To determine how the dynamics of the polypeptide chain in a protein molecule are coupled to the bulk solvent viscosity, the unfolding by urea of the small protein barstar was studied in the presence of two viscosogens, xylose and glycerol. Thermodynamic studies of unfolding show that both viscosogens stabilize barstar by a preferential hydration mechanism, and that viscosogen and urea act independently on protein stability. Kinetic studies of unfolding show that while the rate-limiting conformational change during unfolding is dependent on the bulk solvent viscosity, η , its rate does not show an inverse dependence on η , as expected by Kramers' theory. Instead, the rate is found to be inversely proportional to an effective viscosity, $\eta + \xi$, where ξ is an adjustable parameter which needs to be included in the rate equation. ξ is found to have a value of -0.7 cP in xylose and -0.5 cP in glycerol, in the case of unfolding, at constant urea concentration as well as under isostability conditions. Hence, the unfolding protein chain does not experience the bulk solvent viscosity, but instead an effective solvent viscosity, which is lower than the bulk solvent viscosity by either 0.7 cP or 0.5 cP. A second important result is the validation of the isostability assumption, commonly used in protein folding studies but hitherto untested, according to which if a certain concentration of urea can nullify the effect of a certain concentration of viscosogen on stability, then the same concentrations of urea and viscosogen will also not perturb the free energy of activation of the unfolding of the protein.

© 2006 Elsevier Ltd. All rights reserved.

Keywords: diffusional barrier; internal friction; bulk solvent viscosity; isostability condition; Kramers' theory

*Corresponding author

Introduction

The processes of protein folding and unfolding are transitions between an extended unfolded state and a compact native state, and hence, must involve substantial diffusive motion of the polypeptide chain. During folding, large-scale diffusive motion occurs during the initial collapse event^{1–6} that greatly reduces the conformational space accessible for the polypeptide chain to explore. The diffusive motion of the polypeptide chain is expected to continue as the polypeptide chain surmounts the largely entropic barrier that slows down a protein folding or unfolding reaction. The diffusive dynamics are expected to be dampened by hydrodynamic coupling of the movement of the polypeptide chain

to that of solvent molecules, and several studies have investigated how friction between the polypeptide chain and solvent molecules modulates the passage of protein molecules over the rate-limiting barrier.^{7–18} The motions of different segments of the polypeptide chain may also be coupled to each other during passage over the energy barrier, especially when the chain is transitioning between compact partially structured intermediate forms¹⁹ or when the protein molecule is substantially compact while crossing the energy barrier. Such coupling can give rise to significant internal friction capable of slowing down the structural transition. Even in the absence of a significant energy barrier, which may be true for polypeptide chain collapse during folding²⁰ friction between chain and solvent is expected to play a dominant role in determining the speed of the folding or unfolding reaction. Hence, it is critical to understand better the role of friction in controlling the speed of protein folding or unfolding.

Much of the investigation of the role of friction during protein folding and unfolding has been based on examining the effect of solvent viscosity on the rates

Present address: L. Pradeep, Baker Laboratory of Chemistry, Cornell University, Ithaca NY 14853, USA.

E-mail address of the corresponding author:
jayant@ncbs.res.in

of the structural transitions, and analyzing the effect using Kramers' theory.^{21–24} Kramers' theory describes the crossing of the energy barrier, the transition state, as a diffusive process, dictated by Brownian motion of the chain as a result of collisions with solvent molecules. Standard transition state theory, in which solvent dynamics play no part, postulates that when a protein molecule is poised at the transition state, it will necessarily proceed in the forward direction, even though the theory itself is based on the establishment of a quasi-equilibrium between the ground and transition states. On the other hand, Kramers' theory assumes that barrier crossing occurs through Brownian motion of the polypeptide chain; hence, the barrier can be crossed several times during the transition when friction is high. Consequently, Kramers' theory predicts that the rate of a protein folding or unfolding reaction should scale inversely with friction with the solvent, and hence, on solvent viscosity, provided that the internal friction of the protein chain remains small in comparison. This prediction by Kramers' theory is met in the case of the folding and unfolding reactions of a few proteins,^{25,26} while for other proteins^{11,13,16,27} modifications of Kramers' theory work well in describing the effect of change in solvent viscosity on folding or unfolding kinetics.

In experimental studies of the effect of viscosity on folding or unfolding kinetics, viscosity is typically varied by the addition of a co-solvent (viscogen) such as sucrose, xylose, glycerol or glycols. But viscogenic additives increase not only the solvent viscosity but also protein stability.²⁸ This complicates analysis because the increase in stability will correlate with an increase in folding rate and/or a decrease in unfolding rate. Hence, the stabilizing effect will counteract any effect of viscosity during folding, and enhance any effect of viscosity during unfolding. This problem is circumvented typically by measuring the viscosity dependence of the folding/unfolding kinetics under conditions that confer identical stability, that is, under isostability conditions, which are achieved by adding a denaturant to neutralize the stabilizing effect of the added viscogen. Formal validation of the isostability approach remains, however, to be established for any protein. This is important to do because even though it continues to be utilized in studies of the effect of viscosity on the folding of proteins,^{11,13} the validity of the isostability approach has been questioned.¹⁶ Validation of the isostability approach is important also because many aspects of the effect of a change in viscosity remain unexplained.^{11,13,16,27} For example for some proteins, the ratio of the relative unfolding or refolding time constant in the presence of viscogen to that in its absence, τ/τ_0 , does not scale linearly with the relative solvent viscosity, η/η_0 , with a slope of unity. In such cases, extensions, largely empirical, of Kramers' theory have been used to describe the data.¹⁸

Here the effect of viscosity on the unfolding of the small, single-domain protein barstar has been studied. Barstar functions as the natural inhibitor

of barnase in the bacterium *Bacillus amyloliquefaciens*, and its folding and unfolding pathways have been studied extensively.^{1,29–35} To find out whether the unfolding of barstar is limited in rate by chain diffusion through the solvent, the dependence of the solvent viscosity on its unfolding kinetics has been measured at fixed concentrations of denaturant, and also under isostability conditions, using xylose and glycerol as viscogens.

It is shown that denaturant and viscogen act independently on protein stability, and the dependences of protein stability as well as unfolding rate on denaturant and viscogen concentration have been determined. The unfolding rate of barstar is decelerated significantly in the presence of xylose and glycerol. τ/τ_0 is found not to vary linearly with η/η_0 when xylose was used as the viscogen. The plot of τ/τ_0 versus η/η_0 is linear when glycerol is used as the viscogen, but the slope is not equal to 1. It therefore appears that the protein motions during the rate-limiting step of unfolding are not dampened by the bulk viscosity, but by an effective viscosity that is significantly less than the bulk viscosity, by different amounts for the different viscogens used. It has been possible to validate the basic tenet of the commonly used isostability approach, that a mutually nullifying effect of viscogen and denaturant on native state stability occurs in concert with a mutually nullifying effect of viscogen and denaturant on transition state stability.

Results

Stabilizing effect of xylose and glycerol on barstar

Xylose and glycerol not only increase the viscosity of the solvent, but they also stabilize barstar. Urea-induced unfolding transitions of barstar were carried out in the presence and absence of xylose (in the range of 0–1 M) and glycerol (in the range of 0–24%), using tryptophan emission at 320 nm as the global probe. The data were fit to equation (6) assuming a two-state N \leftrightarrow U transition. Figure 1 shows the dependence of ΔG_{UN}^e , m_u^e and C_m on the concentration of xylose and glycerol. The free energy of unfolding is seen to increase linearly from a value of 4.9 kcal mol⁻¹ in the absence of viscogen to a value of 5.9 kcal mol⁻¹ in 1 M xylose, and to a value of 7.2 kcal mol⁻¹ in 24% glycerol (Figure 1(a) and (d)). The midpoint of the unfolding transition of barstar increased from 4.1 M urea in the absence of viscogen to 5.0 M urea in the presence of 1.0 M xylose, and to 6.15 M urea in the presence of 24% glycerol (Figure 1(c) and (f)). The value of m_u^e is -1.185 kcal mol⁻¹ M⁻¹ in the absence of viscogen, and remains unchanged with the increase in concentration of xylose or glycerol (Figure 1(b) and (e)); the values at all concentrations of xylose and glycerol are within three standard deviations of the value obtained in the absence of an additive, in support of the assumptions made in equation (5).

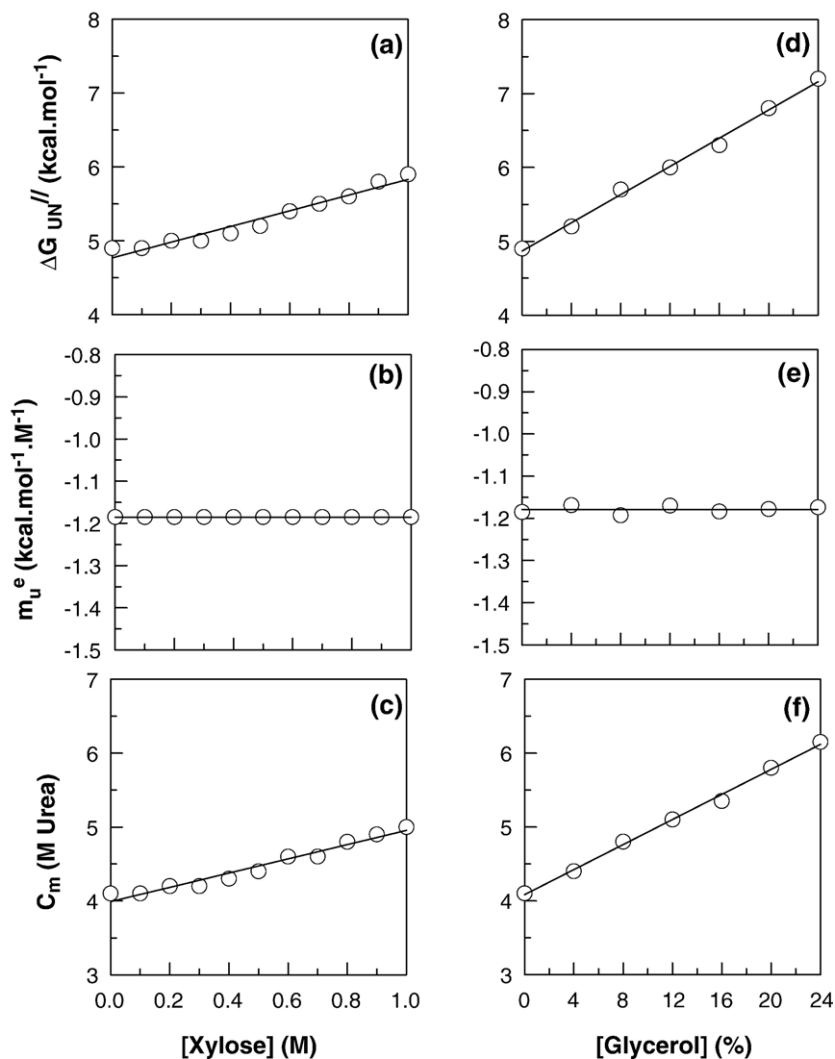


Figure 1. Effect of xylose and glycerol on the thermodynamics of unfolding. (a) ΔG_{UN} , (b) m_u^e and (c) C_m determined from urea-induced unfolding transitions of barstar in xylose at pH 8, 25 °C, monitored by fluorescence at 320 nm upon excitation at 295 nm. (d) ΔG_{UN} , (e) m_u^e and (f) C_m determined from urea-induced unfolding transitions of barstar in glycerol at pH 8, 25 °C, monitored by fluorescence. The continuous line through the data in (a) is a fit of the data to equation (4) and yields values for ΔG_{UN} and m_V^e of 4.8 kcal mol⁻¹ and 1.06 kcal mol⁻¹ M⁻¹, respectively; the continuous line through the data in (b) represents the mean value of m_{UN}^e , (-1.18 kcal mol⁻¹ M⁻¹), averaged over all xylose concentrations; and the continuous line through the data in (c) is described by, $C_{m(\text{xylose})} = 4.0 + 0.96[\text{xylose}]$. The continuous line through the data in (d) is a fit of the data to equation (4) and yields values for ΔG_{UN} and m_V^e of 4.9 kcal mol⁻¹ and 0.096 kcal mol⁻¹ M⁻¹, respectively; the continuous line through the data in (e) represents the mean value of m_{UN}^e , (-1.18 kcal mol⁻¹ M⁻¹), averaged over all glycerol concentrations; and the continuous line through the data in (f) is described by, $C_{m(\text{glycerol})} = 4.1 + 0.085[\text{glycerol}]$.

The observation that the value of m_u^e is not affected by the presence of xylose or glycerol suggests that the urea and either viscogen act independent of each other. The linear dependence of the free energy of unfolding on the concentration of xylose and glycerol was fit to equation (4), which yielded a value of 1.06 kcal mol⁻¹ M⁻¹ for m_V^e (xylose) and a value of 0.096 kcal mol⁻¹ %⁻¹ for m_V^e (glycerol). This increase in stability has to be considered while analyzing the retardation of the unfolding rates by xylose and glycerol.

Dependence of the solvent viscosity on xylose and glycerol concentrations

The viscosities, η , of solutions containing xylose in the concentration range of 0 to 2 M, or glycerol in the concentration range 0 to 30% are plotted against the respective viscogen concentration in Figure 2 and the data fitted to equation (7). The dependence of solvent viscosity on viscogen concentration fits to a simple exponential function, with an exponential coefficient of 0.42 M⁻¹ for xylose (Figure 2(a)) and 0.033%⁻¹ for glycerol (Figure 2(b)). The dependence of solvent viscosity on xylose concentration in the

presence of 7.2 M urea (unfolding condition) also fits to a simple exponential function (equation (7)), with an exponential coefficient of 0.55 M⁻¹ (inset, Figure 2(a)).

Increase in xylose concentration decelerates the unfolding of barstar

Figure 3 shows the kinetics of unfolding of barstar in 7.2 M urea measured by fluorescence at 320 nm, as a function of xylose concentration. The entire process of unfolding is observable at any xylose concentration, and the fast unfolding rate constant decreases with an increase in the concentration of xylose (Figure 3(a)). When unfolding is carried out in ≤ 0.5 M xylose, the unfolding kinetics are described by a single-exponential equation, because the final unfolding condition (7.2 M urea) lies in the post-transition zone of the equilibrium unfolding transitions in the presence of ≤ 0.5 M xylose. The kinetics of unfolding in ≥ 0.6 M xylose, are described by a two-exponential equation (equation (8)), because equilibrium unfolding transitions in the presence of ≥ 0.6 M xylose indicate that a concentration of 7.2 M urea corresponds to a concentration

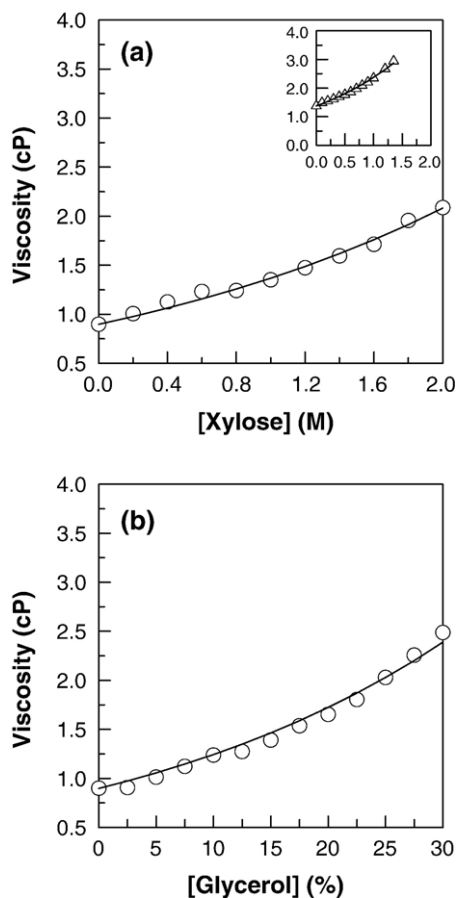


Figure 2. Effect of xylose and glycerol concentration on viscosity of the solvent; (a) viscosity of the solvent with increasing xylose concentration in water and 7.2 M urea (inset) and (b) viscosity of the solvent with increasing glycerol concentration in water. The continuous line through the data in (a), inset of (a), and (b) is a fit of the data to a simple exponential equation (equation (7)), and yields values of 0.42 M^{-1} , 0.55 M^{-1} and $0.033\%^{-1}$, respectively, for the exponential coefficient, c .

in the transition zone. The relative amplitudes of the fast phase of unfolding decrease with an increase in xylose concentration, and the relative amplitude of the slow phase increases with an increase in xylose concentration (Figure 3(b)).

Figure 3(c) shows the dependence of the fast apparent unfolding rate constant on xylose concentration. To determine whether the data satisfied the viscosity dependence predicted by Kramers' theory, the dependence was fit to equation (16). The fit to equation (16) (Figure 3(c)) is not satisfactory, indicating that Kramers' theory cannot adequately describe the viscosity dependence of the apparent unfolding rates.

The inadequacy of Kramers' theory ($k \propto 1/\eta$) is further illustrated in Figure 4, in which the ratio of the unfolding time constant in the presence of viscogen to that in its absence ($\tau_{u,v}/\tau_u$) is plotted against the relative viscosity (η/η_0), for unfolding rates determined under isostability conditions. Isostability conditions were achieved by balancing the

increase in viscogen concentration with an increase in urea concentration, so that all unfolding reactions were carried out in conditions where ΔG_{UN}^{\ddagger} (equation (5)) has a constant value of $-2.25 \text{ kcal mol}^{-1}$. If the assumption that under isostability conditions, the value of the free energy of activation is also not perturbed, is correct and if Kramers' theory is adequate, then the plot of $k_{u,v}/k_u$ versus η_0/η or, $\tau_{u,v}/\tau_u$ versus η/η_0 should be linear according to equation (25), with a slope of 1. Such a plot for glycerol is indeed linear, but the slope is not equal to 1 (Figure 4(b)). Such a plot for unfolding rates determined in different xylose concentrations is not linear but fits to a second-order polynomial equation (Figure 4(a)). The data in Figure 4 therefore indicate that either the isostability assumption is incorrect or that Kramers' theory is not valid for describing the unfolding data or that the unfolding reaction is not a simple single-step reaction.

When deviations from the viscosity dependence predicted by Kramers' theory are seen, data are usually fitted to the phenomenological relationship of equation (9). Equation (9) has two adjustable parameters, p and ξ , and when Kramers' theory is valid, the values of p and ξ are 1 and 0, respectively.

The data in Figure 3(c) were therefore fit to equations (12) and (15). Equation (12) includes the parameter, η_0 , which is the viscosity of the unfolding protein solution not containing any xylose. It has been shown that at high denaturant concentrations, the viscosity is very different from that of a solution where denaturant is either absent or present in low concentrations.^{19,36} Since unfolding was carried out in 7.2 M urea containing different concentrations of xylose, the viscosity of a 7.2 M urea solution was used as the value of η_0 . In equation (12), the adjustable parameter p , is set to 1 so that the only extension to Kramers' theory is the inclusion of the parameter ξ . The data in Figure 3(c) fit well to equation (12) and the fit yielded values for m_v^k and ξ of $0.13 \text{ kcal mol}^{-1} \text{ M}^{-1}$ and -0.74 cP ($\sim -0.7 \text{ cP}$), respectively. On the other hand, the fit to equation (15), in which the adjustable parameter ξ is set to 0, is as unsatisfactory as the fit to equation (16), in which $\xi=0$ and $p=1$ (in fact, the two fits overlap). This indicates that allowing the value of p to vary from 1 is not necessary or appropriate.

The value of $0.13 \text{ kcal mol}^{-1} \text{ M}^{-1}$ obtained for m_v^k from the fit to equation (12) can be used to check the validity of the isostability assumption that under conditions where the concentrations of urea and viscogen are such that the value of ΔG_{UN}^{\ddagger} is kept constant, the same concentrations of urea and viscogen will also ensure that the value of the free energy of activation for unfolding will remain constant. If this assumption is correct, then the relationship between the m values, described by equation (21), must hold true. The value of m_v^e (xylose) has been determined from Figure 1(a) to be $1.06 \text{ kcal mol}^{-1} \text{ M}^{-1}$, the value of m_u^e is known from previous studies³² to be $-1.16 \text{ kcal mol}^{-1} \text{ M}^{-1}$, and the value of m_u^k is known from previous studies³² to be $-0.14 \text{ kcal mol}^{-1} \text{ M}^{-1}$ (see also Materials and

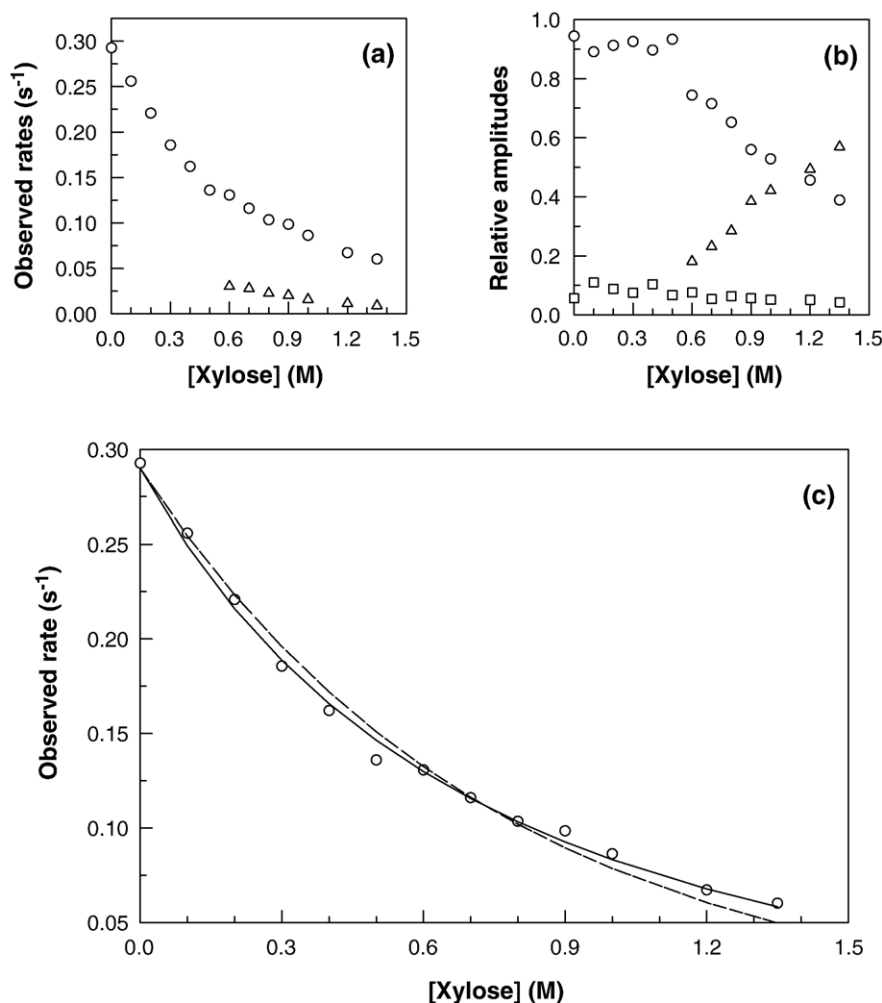


Figure 3. Dependence of the apparent unfolding rates on xylose concentration at constant urea concentration. (a) Dependence of the fast (○) and slow (Δ) unfolding rate constants on xylose concentration during unfolding in 7.2 M urea (pH 8). (b) Dependence of the relative amplitudes of the fast (○) and slow (Δ) phases during unfolding in 7.2 M urea (pH 8). The complete process of unfolding is observed at any xylose concentration and the relative amplitude of the burst phase (□) is essentially zero. (c) Dependence of the fast unfolding rate constants, λ_2 , (○) on xylose concentration during unfolding in 7.2 M urea (pH 8). The dotted line is a least-squares fit of the data to equation (16) and yields values of $0.45 \text{ kcal mol}^{-1} \text{ M}^{-1}$ for m_V^k . The continuous line is a fit of the data to equation (12) and yields values of $0.13 \text{ kcal mol}^{-1} \text{ M}^{-1}$ and -0.74 cP for m_V^k and ξ , respectively. The broken line is a fit of the data to equation (15) and yields values of $0.73 \text{ kcal mol}^{-1} \text{ M}^{-1}$ and 0.14 for m_V^k and p , respectively. The dotted line is completely hidden under the broken line. In all fits, the value of k_u was fixed at 0.29 s^{-1} , which is the value of the apparent unfolding rate constant in 7.2 M urea in the absence of any xylose; the value of η_0 was fixed at 1.37 cP , which is the

viscosity determined for a 7.2 M urea solution (Figure 2(a), inset); and, the value of the exponential coefficient, c , was fixed at 0.55 M^{-1} (inset of Figure 2(a)).

Methods). According to equation (21), the value of m_V^k (xylose) should therefore be $0.13 \text{ kcal mol}^{-1} \text{ M}^{-1}$, for the isostability assumption to be valid. This is exactly the value obtained for m_V^k (xylose) from the fit of the data in Figure 3(c) to equation (12). Thus, it appears that the isostability assumption is true for the unfolding of barstar.

This validation of the isostability assumption means that the apparent unfolding rates determined under an isostability condition, such as shown in Figure 4, can be analyzed according to equation (24). Figure 5 shows the apparent fast unfolding rate determined under an isostability condition ($\Delta G_{UN}^{\ddagger} = -2.25 \text{ kcal mol}^{-1}$) at different concentrations of xylose (Figure 5(a)) and glycerol (Figure 5(b)). A fit of the data in Figure 5(a) to equation (24) yields a value of ξ of -0.66 cP ($\sim -0.7 \text{ cP}$) for unfolding in xylose. This value of ξ is similar to the value obtained from fitting the data of Figure 3(c), -0.74 cP ($\sim -0.7 \text{ cP}$), which was obtained at a fixed urea concentration of 7.2 M, to equation (12). This result again validates the isostability assumption. A fit of the data in Figure 5(b) for unfolding in glycerol provides a value of -0.49 cP for unfolding in

glycerol, which is different from the value obtained for unfolding in xylose.

Discussion

Interpretation of ξ as an internal friction term

It has been very difficult to interpret the viscosity dependence of protein folding and unfolding, and only a small number of studies of the viscosity dependencies of protein conformational changes have been reported. For example, in the study of CO-haemoglobin, a slope of <1 was found for the CO dynamics.⁹ This subunitary value was attributed to attenuation and transformation of the effect of the cosolvent on internal protein dynamics.³⁷ Similar observations have been reported for other systems as well.³⁸ A distinction between internal friction and solvent friction was used in the interpretation of the conformational relaxation of myoglobin.⁹ The refolding kinetics displayed a Kramers'-like viscosity dependence only at high viscosities ($\sim 20 \text{ cP}$). The data were analyzed by partitioning the friction term

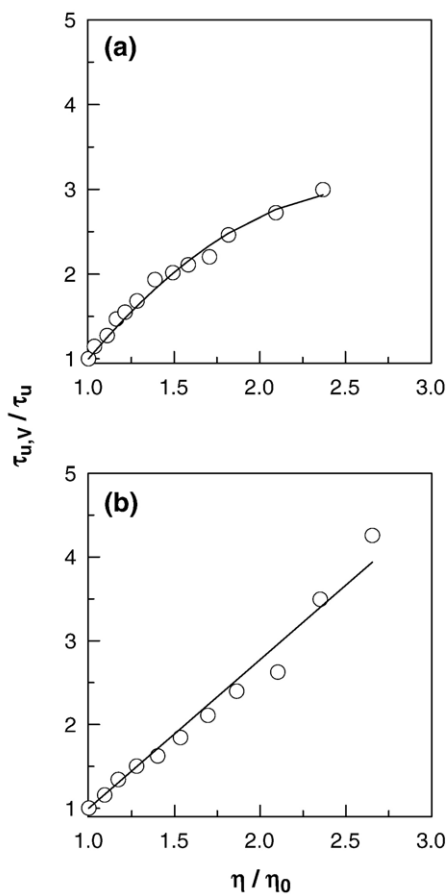


Figure 4. Dependence of the relative unfolding time constant on the relative viscosity of the solution, under isostability condition ($\Delta G_{UN}^{///} = -2.25$ kcal mol⁻¹). (a) The apparent unfolding time constant of barstar in xylose relative to the unfolding time constant in the absence of xylose, $\tau_{u,v}/\tau_u$ versus η/η_0 . The final urea concentration upon unfolding was varied from 6.0 M to 7.25 M to maintain a constant native state stability of -2.25 kcal mol⁻¹. The continuous line is a fit of the data to a second order polynomial equation, $\tau_{u,v}/\tau_u = -2.13 + 3.86(\eta/\eta_0) - 0.73(\eta/\eta_0)^2$. Error bars on the points are standard deviations from three separate determinations, and are smaller than the size of the symbols used. (b) The unfolding rate constant of barstar in glycerol relative to the unfolding rate constant in the absence of glycerol, $\tau_{u,v}/\tau_u$ versus η/η_0 . The final urea concentration upon unfolding was varied from 6.0 M to 7.7 M to maintain a constant native state stability of -2.25 kcal mol⁻¹. The continuous line is a fit of the data to a linear equation and yields a slope of 1.78. Error bars on the points are smaller than the size of the symbols used, and are standard deviations from four separate determinations. For the transformation of the data in both panels, the viscosity of a 6 M urea solution was taken as the value of η_0 (1.24 cP), because this urea concentration maintains isostability conditions in the absence of viscogen. The viscosity of each viscogen-containing solution was independently measured to obtain the value of η , and hence, η/η_0 , for that solution.

into an internal and solvent friction component. This was done by interpreting the adjustable parameter ξ of equation (9) as internal friction. In this interpretation of ξ , it is supposed to represent the internal

friction between segments of the polypeptide chain as it folds, similar to the relative sliding of layers of solvent molecules in viscous liquids.

A protein folds independently of solvent viscosity, when the internal friction of the protein chain in the transition state is much higher than the friction with the solvent molecules. This internal friction is not constant for proteins. For CspB^{11,15} and protein L,¹³

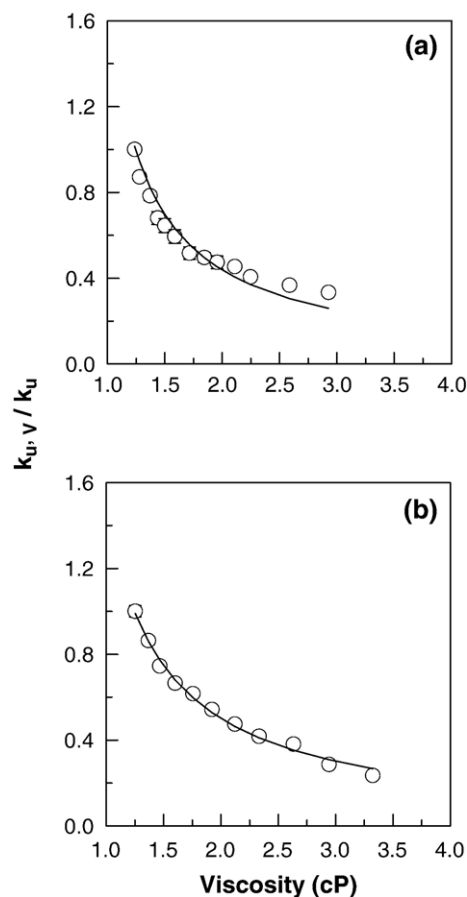


Figure 5. Dependence of the relative unfolding rate constant on the viscosity of the solution, under isostability condition. For each viscogen-containing solution, the viscosity, η , was determined independently. (a) The unfolding rate constant of barstar in xylose relative to the unfolding rate constant in the absence of xylose, $k_{u,v}/k_u$ versus viscosity η at each isostability condition. The final urea concentration upon unfolding was varied from 6.0 M to 7.25 M to maintain a constant native state stability of -2.25 kcal mol⁻¹. The continuous line is a fit of the data to equation (24), with the value of η_0 fixed at 1.24 cP (the viscosity of a 6 M urea solution; see the legend to Figure 4), and yields a value of -0.66 cP for ξ . Error bars on the points are standard deviations from three separate determinations. (b) The unfolding rate constant of barstar in glycerol relative to the unfolding rate constant in the absence of glycerol, $k_{u,v}/k_u$ versus viscosity η at each isostability condition. The final urea concentration upon unfolding was varied from 6.0 M to 7.7 M to maintain a constant native state stability of -2.25 kcal mol⁻¹. The continuous line is a fit of the data to equation (24), with the value of η_0 fixed at 1.24 cP (the viscosity of a 6 M urea solution), and yields a value of -0.49 cP for ξ . Error bars on the points are standard deviations from four separate determinations.

the internal viscosity is lower than the viscosity of the surrounding solvent when the activation barrier is crossed, and hence, is not relevant as a rate-limiting factor. But, for many proteins, the internal viscosity increases early during the folding reaction, particularly when the intermediates are formed, and becomes higher than the friction with the solvent when the transition state is traversed. In such a case, folding becomes independent of solvent viscosity, as is seen for α lactalbumin.¹¹ An increase in internal viscosity friction, thus contributes to kinetic traps on folding routes. A low value for internal friction is interpreted to mean that the protein chain can move rather freely. When the protein is densely packed, the chain segments can possibly no longer slide freely along energy trajectories, but instead jump between discrete conformational substates, separated by sizable energy barriers. In such cases, the internal viscosity and the size of the energy barrier can be correlated, because they both originate from the hindered movement of chain segments relative to one another in the transition state.¹⁷

A modification of Kramers' theory has been used to fit the end-to-end diffusion kinetics of polyglycine chains ranging from four to ten residues,³⁹ where the dynamics of the ten-residue chain are inversely dependent on solvent viscosity and the dynamics of the four-residue chain by contrast, are dominated by an internal friction component, and is affected relatively less by changing solvent viscosity. The viscosity dependence of the rate of ligand dissociation-induced conformational changes in myoglobin indicates that for the structural rearrangements of a compact, solvent-excluded, native protein, an internal friction term, ξ , approximately four times that of water, plays a major role.⁹ The viscosity dependence of refolding of several proteins^{17,38,39} is best accounted for by including the ξ term in the analyses of the viscosity dependences of their folding. On the other hand, a simple proportional relationship between refolding time constants and relative viscosity for protein L¹³ under isostability conditions has shown that the refolding of protein L does not exhibit a significant internal friction component. Similarly, it has been shown from studies of unfolding and refolding of CspB at isostability conditions, that τ/τ_0 varies linearly with η/η_0 with a unitary slope. The inclusion of an internal friction component is not required, suggesting that the collapse of the polypeptide chain occurs in the rate-limiting step during its folding.^{11,15} There has been no report which required the inclusion of the ξ term in the analyzing of the viscosity dependence of the unfolding of a protein. In the two studies on the viscosity dependence of unfolding kinetics,^{8,11} τ/τ_0 was found to vary linearly with η/η_0 exhibiting a slope of 1. There was no need for the inclusion of the ξ term.

Kramers' theory and the unfolding of barstar

In this study when the apparent unfolding rates of barstar in the presence of xylose, at constant urea concentration (Figure 3(c)) were fitted to equation

(16), an equation which does not include the adjustable parameter ξ , the fit to the data was not good, indicating that Kramers' theory was not adequate to explain the unfolding reaction of barstar. Two extensions to Kramers' theory were therefore considered in which the adjustable parameters ξ and p are included (equation (9)). Fitting the data in Figure 3(c) to equation (15), which lacks the ξ term, but includes the parameter, p , not equal to 1 (for reactions satisfying Kramers' theory, $p=1$) also yields a poor fit, indicating that an extension of Kramers' theory which includes only the parameter p is inadequate to explain the data. A fit to equation (12), in which only the adjustable parameter ξ is included in the extension of Kramers' theory, is, however, satisfactory (Figure 3(c)). But the value obtained for ξ is negative.

Barstar does not experience bulk solvent viscosity during unfolding

The negative values of ~ -0.7 cP and ~ -0.5 cP for ξ obtained from an analysis of the unfolding of barstar in the presence of xylose and glycerol, respectively, suggest that the usual interpretation of ξ as denoting internal protein friction is not correct in the case of the unfolding of barstar. Here, ξ appears to be a viscosity term denoting the extent to which the effective viscosity, that actually dampens the motions of the protein chain as it unfolds, is lower than the bulk solvent viscosity. The negative value of ξ indicates that the motions of the protein chain are not dampened by the bulk solvent viscosity η but by an effective solvent viscosity $\eta + \xi$.

At this stage, it is not clear as to why the protein does not feel the bulk solvent viscosity. Perhaps the explanation lies in the mode of interaction of xylose and glycerol with the protein. The thermodynamic analyses of the interaction of either of these cosolvents with barstar (Figure 1) indicates that the mode of interaction is through a preferential hydration mechanism²⁸ because the free energy of stabilization of N with respect to U has a linear dependence^{12,28,40} on the concentration of either xylose or glycerol. According to the mechanism of preferential hydration, the protein is surrounded by a shell of water molecules from which cosolvent molecules, such as of xylose and glycerol used here, are preferentially excluded⁴⁰⁻⁴² because of surface tension. The presence of a shell of water molecules separating the protein molecules from bulk solvent will mean that the motions of the protein chain as it unfolds will be dampened not by bulk viscosity but by an effective viscosity that is lower than the bulk viscosity by the quantity ξ .

There is considerable evidence for the presence of a bound water layer or hydration shell on the surface of a native protein in solution.⁴³⁻⁴⁹ Precise measurements of the diffusion coefficients of molecules as large as protein molecules, which are large compared to the size of water molecules, have validated the Stoke-Einstein relation, which says that diffusional motion is inversely proportional to

solvent viscosity.⁵⁰ These measurements have also shown that the Stokes radius for large molecules is larger than the radius computed from the partial molar volume by $\sim 15\%$, presumably because of a tightly bound water layer which migrates with the protein, although protein shape may also play a role.⁴⁸ Characterization of the ultrafast dynamics of the bound water molecules by time-resolved fluorescence spectroscopy^{47,49} indicate that the water molecules in the bound water layer around a folded protein exist in rigid but ephemeral structures that are lost upon unfolding of the protein. X-ray and neutron scattering studies indicate that the density of the hydration shell is significantly more than that of bulk water.⁴⁵

There is some controversy about the local viscosity in the hydration shell. Magnetic dispersion experiments indicate that the local viscosity is higher than the bulk solvent viscosity, but these studies also indicate a highly mobile hydration layer,⁴⁸ a result incompatible with that of time-resolved fluorescence measurements of ultrafast dynamics.^{47,49} On the other hand, kinetic measurements of CO binding to myoglobin have suggested that the local viscosity at the protein-solvent interface is smaller than the bulk solvent viscosity.¹⁴ Time resolved fluorescence anisotropy decay studies⁵¹ have also shown that the rotational dynamics of solvent-exposed tryptophan side-chains are dampened not by the bulk solvent viscosity but by a lower effective viscosity. Moreover, the rotational dynamics are less sensitive to bulk solvent viscosity in native proteins than they are in unfolded proteins, suggesting the presence of water bound to proteins in their folded but not unfolded states. It appears that an unfolded protein molecule may be similar to a small solute molecule in not possessing a bound water layer⁵⁰ and it is noteworthy for small solute molecules that although the diffusional coefficient varies inversely with viscosity, the slope may be either greater or smaller than 1.⁵⁰ In this context, it is possible that the motions of only very small segments of the poly-

peptide chain are involved in the rate-limiting step of unfolding.

It is likely that it is the bound water layer on a folded protein molecule which controls the dynamics of the protein chain and side-chains, including the motions associated with protein unfolding, and which insulates the protein from the bulk solvent. This is depicted pictorially in Figure 6. Of course, during unfolding, the protein structure itself might also affect the hydrodynamic coupling of the polypeptide chain in the protein interior with the solvent.

Validation of the isostability approach

The isostability approach was introduced originally by Chrnyk and Matthews when they investigated domain pairing in the folding of the α subunit of tryptophan synthase.⁸ Subsequently, the utility of this approach has been demonstrated in folding and unfolding studies of CspB¹¹ and protein L,¹³ where the folding rates scale linearly with viscosity with a near-unitary slope.^{8,11,13} Moreover, the retardation of folding rates was seen to be independent of the chemical nature of the viscogenic agent, as also seen here. In the case of CspB¹¹ and the α subunit of tryptophan synthase⁸ the unfolding rates were observed to scale linearly with viscosity with a near-unitary slope.^{8,11} Thus, even though denaturant and viscogen might affect protein stability by different mechanisms,¹⁶ the isostability approach seems to work well. Also, when the progressively larger, stabilizing effect of increasing concentration of the added viscogen could be negated, as it is when the viscogen ethylene glycol is used at higher temperature,^{15,52} the effect of increasing viscosity on folding rate could be shown to follow Kramers' theory.

In spite of the utility of the isostability approach, there has never been explicit validation of a basic tenet of the approach, namely that when the stabilizing effect of the viscogen is counterbalanced

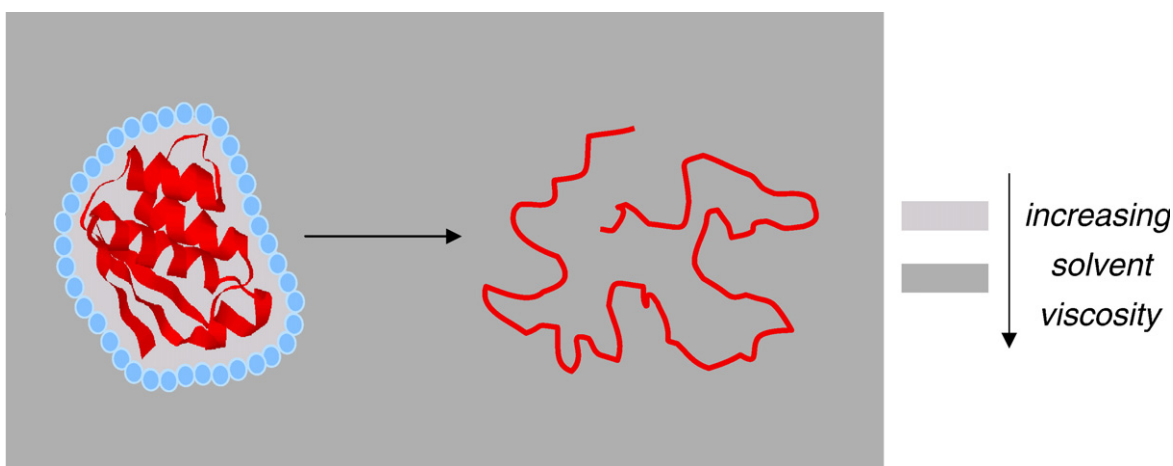


Figure 6. Pictorial representation of the bound water layer or hydration shell on the surface of the native protein in solution. The motions of the protein chain as it unfolds are dampened by an effective viscosity $\eta+\xi$ and not the bulk viscosity η , the effective viscosity being lower than the bulk viscosity by the quantity ξ .

exactly by the destabilizing effect of denaturant, this mutual neutralization of effects acts not only on native state stability, but also in an identical manner on transition state stability. In this study of the effect of viscosity on the unfolding of barstar, this basic tenet has been validated.

Materials and Methods

Bacterial strain and plasmid, and protein purification

The *Escherichia coli* strain MM294 was used for protein expression. The expression plasmid for wt barstar was pMT316 provided by R. W. Hartley. The method used to purify barstar has been described in detail.⁵³ Protein concentrations were calculated using an extinction coefficient of $23,000 \text{ M}^{-1}\text{cm}^{-1}$.⁵³ Mass spectroscopy using a Micromass Q-TOF Ultima showed that the protein was pure with a mass of 10,342, which indicated that the N-terminal methionine residue had remained uncleaved during synthesis.

Materials

Tris-HCl (ultrapure, 99.9%) and DTT (ultrapure) were from GibcoBRL; EDTA disodium salt (ultrapure, 99+%), xylose (ultrapure, 99%) and glycerol (ultrapure, 99%) were from SIGMA; and urea (ultrapure) was from USB.

Buffers and solutions

30 mM Tris-HCl (pH 8), 250 μM EDTA and 250 μM DTT (ultrapure from GibcoBRL) constituted the native buffer used for all equilibrium experiments. Unfolding buffer was native buffer containing 9 to 10 M urea. The concentrations of stock solutions of urea were determined by measuring the refractive index using an Abbe 3L refractometer from Milton Roy. For urea-induced equilibrium denaturation studies in the presence of viscogen (xylose or glycerol), the viscogen was present in the refolding as well as unfolding buffer; up to 1 M xylose or up to 24% (v/v) glycerol was present. All buffers and solutions were filtered through 0.22 μm filters before use.

For refolding kinetic experiments, 30 mM Tris-HCl, 250 μM EDTA, 250 μM DTT, with or without 2.2 M xylose constituted the two native buffers. 30 mM Tris-HCl, 250 μM EDTA, 250 μM DTT and 9 M urea constituted the unfolding buffer; the unfolding buffer did not contain any xylose. The protein was unfolded at least 4 h prior to the refolding experiments. Appropriate dilutions of the three buffers were made on the stopped-flow mixing module to give the final desired xylose and urea concentration; the urea concentration was constant at 0.9 M during refolding, whereas the xylose concentration was varied from 0 to 2.0 M. All buffers and solutions were filtered through 0.22 μm filters before use. The experiments were carried out at 25 °C.

For unfolding experiments, 30 mM Tris-HCl (pH 8), 250 μM EDTA and 250 μM DTT constituted the native buffer. The unfolding buffer was native buffer containing 8 M urea. Upon unfolding, the final urea concentration was maintained constant at 7.2 M urea. Xylose was present in the refolding as well as the unfolding buffers up to a concentration of 1 M. Unfolding in the presence of varying concentrations of xylose was studied at constant

urea concentration. All buffers and solutions were filtered through 0.22 μm filters before use and the experiments were carried out at 25 °C.

For unfolding experiments under isostability conditions in the presence of xylose and glycerol, 30 mM Tris-HCl, 250 μM EDTA, 250 μM DTT, constituted the native buffer. 30 mM Tris-HCl, 250 μM EDTA, 250 μM DTT and 8.1 M urea, with or without 1.5 M xylose (or, 8.55 M urea, with or without 22.22% glycerol) constituted the two unfolding buffers. Appropriate dilutions of the three buffers were made on the stopped-flow mixing module to give the final desired urea-xylose/urea-glycerol concentration, such that the net stability of barstar was $-2.25 \text{ kcal mol}^{-1}$. All buffers and solutions were filtered through 0.22 μm filters before use and the experiments carried out at 25 °C.

Viscosity measurements

Viscosity measurements of all the xylose and glycerol solutions, in the presence as well as absence of urea, were made using an Oswald's viscometer. All measurements were made at 25 °C. Viscosity was calculated using the following equation:

$$\eta_{\text{solution}} = \frac{t_{\text{solution}}}{t_{\text{water}}} \times \frac{d_{\text{solution}}}{d_{\text{water}}} \times \eta_{\text{water}} \quad (1)$$

where, t_{solution} and t_{water} are the times of flow of the solution and water, respectively, between the two marks for constant volume on the bulb of the viscometer; d_{solution} and d_{water} are the densities of the solution (determined using equation (2)) and water (known from literature to be $0.9971 \times 10^3 \text{ kg m}^{-3}$ at 25 °C), respectively; and η_{water} is the viscosity of water at 25 °C (known from the literature to be 0.8937 cP). The density of the solution is determined by:

$$d_{\text{solution}} = \frac{\text{weight of the solution}}{\text{weight of the same volume of water}} \times d_{\text{water}} \quad (2)$$

Equilibrium unfolding studies

Protein stability at equilibrium was determined by urea-induced denaturation studies using fluorescence at 320 nm as the probe. Prior to the fluorescence measurements, the samples were equilibrated for at least 4 h. Identical results were obtained if the time of incubation was 24 h. The samples were excited at 295 nm and emission collected at 320 nm, with the band widths as mentioned above.

Kinetic experiments

Kinetic experiments were performed on a Biologic SFM-4 stopped-flow mixing module. Folding and unfolding were monitored using intrinsic tryptophan fluorescence as the probe. The excitation wavelength was set at 295 nm, and emission was monitored at 320 nm using an Oriol bandpass filter with a band width of 10 nm. The protein concentration during refolding and unfolding was between 15 μM and 20 μM . In all experiments, an FC-15 cuvette with a path length of 1.5 mm was used, the total flow rate was 6.0 ml s^{-1} , and the dead time of the instrument was 5.0 ms. For unfolding experiments at constant urea concentration in the presence of increasing amounts of xylose, the final urea concentration upon unfolding was 7.2 M. For unfolding at isostability conditions in the presence of viscogens (xylose and glycerol), the final urea-viscogen concentration upon

unfolding was such that the net stability of barstar was $-2.25 \text{ kcal mol}^{-1}$.

Data analysis

Equilibrium unfolding studies

According to the weak interaction (linear free energy) model for describing the interaction of urea (D) with a protein,^{54,55} the change in free energy, $\Delta G'_{UN}$, that occurs upon unfolding the native protein, N , in the presence of D , is linearly dependent on denaturant concentration, $[D]$:

$$\Delta G'_{UN} = \Delta G_{UN} + m_u^e [D] \quad (3)$$

m_u^e is the change in free energy associated with the preferential interaction of the denaturant with the unfolded form, U , relative to the folded form, N . $\Delta G'_{UN}$ represents the free energy of unfolding of N in the presence of denaturant and ΔG_{UN} represents the free energy of unfolding of N to U in the absence of any denaturant or added co-solute.

A cosolvent such as a viscogen, V , acting as a chemical perturbant, also interacts with a protein according to the weak interaction model^{40,41} and the free energy of unfolding of N to U , in the presence of V , is expected to be linearly dependent on viscogen concentration, $[V]$:

$$\Delta G'_{UN} = \Delta G_{UN} + m_v^e [V] \quad (4)$$

m_v^e is the change in free energy associated with the preferential interaction of the viscogen with the unfolded form, U , relative to the native form, N , in an equilibrium unfolding transition. According to equation (4), m_v^e has a positive value when the folded form is stabilized in the presence of viscogen. $\Delta G'_{UN}$ represents the free energy of stabilization of N , in the presence of viscogen.

Thus, in the presence of both denaturant and viscogen, the free energy of unfolding of N to U , $\Delta G'_{UN}$ is given by:

$$\Delta G'_{UN} = \Delta G_{UN} + m_v^e [V] + m_u^e [D] \quad (5)$$

Equation (5) assumes that m_u^e is independent of $[V]$ and that m_v^e is independent of $[D]$.

Equilibrium data for the unfolding of N as a function of $[D]$, obtained in the presence of a fixed concentration of viscogen, were fit to a two-state $U \leftrightarrow N$ model according to the equation:

$$Y_0 = \frac{Y_N + m_N [D] + (Y_U + m_U [D]) e^{-\frac{(\Delta G'_{UN} + m_u^e [D])}{RT}}}{1 + e^{-\frac{(\Delta G'_{UN} + m_u^e [D])}{RT}}} \quad (6)$$

where Y_0 is the value of the spectroscopic property being measured as a function of $[D]$ at fixed $[V]$, Y_N and Y_U represent the intercepts, and m_N and m_U the slopes, of the native protein and unfolded protein baselines, respectively. Thus, fits of denaturant-induced equilibrium unfolding data at different fixed values of $[V]$ to equation (6), yield values for $\Delta G'_{UN}$ and m_u^e at each fixed $[V]$, and a subsequent fit of the viscogen dependence of $\Delta G'_{UN}$ to equation (4) yields values for ΔG_{UN} and m_v^e .

Dependence of viscosity on the concentration of the viscogen

The simple exponential dependence of the solvent viscosity on the concentration of xylose and glycerol is given by the equation:

$$\eta = \eta_0 e^{c[V]} \quad (7)$$

where η is the solvent viscosity in the presence of the viscogen, η_0 is the viscosity in the absence of any viscogen (either in the absence or the presence of denaturant (urea) D), c is the exponential coefficient and $[V]$ is the concentration of the viscogen.

Kinetic studies

The observable kinetics of unfolding of barstar in 7.2 M urea is described by a two-exponential process in the presence of ≥ 0.6 M xylose:

$$A(t) = A(\infty) + A_1 e^{-\lambda_1 t} + A_2 e^{-\lambda_2 t} \quad (8)$$

or by a single exponential process for unfolding in ≤ 0.5 M xylose, by setting A_1 equal to zero in equation (8). Here, $A(t)$ and $A(\infty)$ are the observed reduced amplitudes at times t and at infinity; λ_1 and λ_2 are the apparent rate constants of the slow and fast phases; and A_1 and A_2 are the respective amplitudes. The relative amplitude of each phase was determined by dividing the observed amplitude of that phase by the equilibrium amplitude of the reaction at 7.2 M urea.

In the limit of high viscosity, Kramers' model predicts that the reaction rates are inversely proportional to η . Extensions of Kramers' theory have been used to describe the conformational dynamics of the protein folding reaction,^{14,17} and one such extension is the inclusion of the adjustable parameter ξ , which, together with the bulk solvent viscosity, η , determines the effective viscosity felt by the protein. Another is the inclusion of the adjustable parameter p , as the exponent of solvent viscosity, η . The reaction rate is then given by the phenomenological equation:

$$k = \frac{\nu}{\eta^p + \xi} e^{-\frac{\Delta G^\ddagger}{RT}} \quad (9)$$

where, ν is a proportionality constant with units of cP^{-1} and ΔG^\ddagger is the free energy barrier.

When η_0 is the viscosity of the denaturant (urea) solution, D , in the absence of any added viscogen, and when $p=1$, equation (9) can be written as:

$$k_u = \frac{\nu}{\eta_0 + \xi} e^{-\frac{(\Delta G_0^\ddagger + m_u^k [D])}{RT}} \quad (10)$$

where $-m_u^k/2.303RT$ is the slope of the plot of logarithm of the unfolding rate constant, k_u , versus denaturant concentration, $[D]$. This slope is known to have a value of 0.105 M^{-1} from earlier studies.³² Thus, m_u^k has a value of $-0.141 \text{ kcal mol}^{-1} \text{ M}^{-1}$.

In the presence of both urea and viscogen, on combining equations (7) and (10), we have:

$$k_{u,V} = \frac{\nu}{\eta_0 e^{c[V]} + \xi} e^{-\frac{(\Delta G_0^\ddagger + m_u^k [D] + m_v^k [V])}{RT}} \quad (11)$$

where c is known from determining the dependence of viscosity on viscogen concentration in the presence of a fixed denaturant concentration (in this case, 7.2 M urea) according to equation (7); $m_v^k/2.303RT$ is the slope of the plot of logarithm of the unfolding rate constant in the presence of viscogen, $k_{u,V}$, versus viscogen concentration, $[V]$, and is not known.

Combining equations (10) and (11):

$$k_{u,V} = k_u \frac{\eta_0 + \xi}{\eta_0 e^{c[V]} + \xi} e^{-\frac{m_v^k [V]}{RT}} \quad (12)$$

where k_u , defined by equation (10) is the unfolding rate constant in the absence of any viscogen, V .

When $\xi=0$ and when $p \neq 1$:

$$k_u = \frac{v}{\eta_0^p} e^{-\frac{(\Delta G_0^\ddagger + m_u^k[D])}{RT}} \quad (13)$$

$$k_{u,V} = \frac{v}{\eta_0^p e^{pc[V]}} e^{-\frac{(\Delta G_0^\ddagger + m_u^k[D] + m_V^k[V])}{RT}} \quad (14)$$

and,

$$k_{u,V} = k_u e^{-\frac{(pcRT[V] + m_V^k[V])}{RT}} \quad (15)$$

When $\xi=0$ and when $p=1$,

$$k_{u,V} = k_u e^{-\frac{(cRT[V] + m_V^k[V])}{RT}} \quad (16)$$

Unfolding under isostability conditions

The assumption is that if the perturbation of the stability of the native state, ΔG_{UN} , by $[V]_I$ is nullified by the addition of $[D]_I$, then, for $U \leftrightarrow TS^\ddagger$ and $TS^\ddagger \leftrightarrow N$, any perturbation of ΔG^\ddagger by the same concentration of V will also be nullified by addition of the same concentration of D .

If, at equilibrium, ΔG_{UN} is not perturbed, equation (5) becomes:

$$\Delta G_{UN} = \Delta G_{UN} + m_V^e[V]_I + m_u^e[D]_I \quad (17)$$

or, in other words:

$$-\frac{m_V^e}{m_u^e} = \frac{[D]_I}{[V]_I} \quad (18)$$

With the isostability assumption, that is, if ΔG^\ddagger is also not perturbed at the same concentrations of D and V :

$$\Delta G^\ddagger = \Delta G^\ddagger + m_V^k[V]_I + m_u^k[D]_I \quad (19)$$

and in other words:

$$-\frac{m_V^k}{m_u^k} = \frac{[D]_I}{[V]_I} \quad (20)$$

If the assumption made above is correct, then on combining equations (18) and (20), we have:

$$\frac{m_V^e}{m_u^e} = \frac{m_V^k}{m_u^k} \quad (21)$$

Testing the validity of equation (21) therefore represents a test of the isostability assumption.

For experiments carried out under isostability conditions, and when the assumption of perturbations on the native state and the transition state being identical, is valid, then, when $p=1$:

$$k_u = \frac{v}{\eta_0 + \xi} e^{-\frac{\Delta G^\ddagger}{RT}} \quad (22)$$

and:

$$k_{u,V} = \frac{v}{\eta + \xi} e^{-\frac{\Delta G^\ddagger}{RT}} \quad (23)$$

On combining equations (22) and (23), we have:

$$\frac{k_{u,V}}{k_u} = \frac{\eta_0 + \xi}{\eta + \xi} \quad (24)$$

When $\xi=0$, then under isostability conditions:

$$\frac{k_{u,V}}{k_u} = \frac{\eta_0}{\eta} \quad (25)$$

Hence, under isostability condition, and when $p=1$ and $\xi=0$, a plot of $k_{u,V}/k_u$ versus η_0/η (or, $\tau_{u,V}/\tau_u$ versus η/η_0) will have a slope of 1.

Acknowledgements

We thank G. Krishnamoorthy for suggestions and discussions; and M. K. Mathew, Kalyan Sinha and Santosh Kumar Jha for their comments on the manuscript. This work was funded by the Tata Institute of Fundamental Research and the Department of Science and Technology, Government of India.

References

1. Agashe, V. R., Shastri, M. C. & Udgaonkar, J. B. (1995). Initial hydrophobic collapse in the folding of barstar. *Nature*, 377, 754–757.
2. Akiyama, S., Takahashi, S., Ishimori, K. & Morishima, I. (2000). Stepwise formation of alpha-helices during cytochrome c folding. *Nature Struct. Biol.* 7, 514–520.
3. Rami, B. R. & Udgaonkar, J. B. (2002). Mechanism of formation of a productive molten globule form of barstar. *Biochemistry*, 41, 1710–1716.
4. Magg, C. & Schmid, F. X. (2004). Rapid collapse precedes the fast two-state folding of the cold shock protein. *J. Mol. Biol.* 335, 1309–1323.
5. Uzawa, T., Akiyama, S., Kimura, T., Takahashi, S., Ishimori, K., Morishima, I. & Fujisawa, T. (2004). Collapse and search dynamics of apomyoglobin folding revealed by submillisecond observations of alpha-helical content and compactness. *Proc. Natl Acad. Sci. USA*, 101, 1171–1176.
6. Kimura, T., Uzawa, T., Ishimori, K., Morishima, I., Takahashi, S., Konno, T. *et al.* (2005). Specific collapse followed by slow hydrogen-bond formation of beta-sheet in the folding of single-chain monellin. *Proc. Natl Acad. Sci. USA*, 102, 2748–2753.
7. Tsong, T. Y. & Baldwin, R. L. (1978). Effects of solvent viscosity and different guanidine salts on the kinetics of ribonuclease A chain folding. *Biopolymers*, 17, 1669–1678.
8. Chrnyk, B. A. & Matthews, C. R. (1990). Role of diffusion in the folding of the alpha subunit of tryptophan synthase from *Escherichia coli*. *Biochemistry*, 29, 2149–2154.
9. Ansari, A., Jones, C. M., Henry, E. R., Hofrichter, J. & Eaton, W. A. (1992). The role of solvent viscosity in the dynamics of protein conformational changes. *Science*, 256, 1796–1798.
10. Waldburger, C. D., Jonsson, T. & Sauer, R. T. (1996). Barriers to protein folding: formation of buried polar interactions is a slow step in acquisition of structure. *Proc. Natl Acad. Sci. USA*, 93, 2629–2634.
11. Jacob, M., Schindler, T., Balbach, J. & Schmid, F. X. (1997). Diffusion control in an elementary protein folding reaction. *Proc. Natl Acad. Sci. USA*, 94, 5622–5627.

12. Creighton, T. E. (1997). Protein folding: does diffusion determine the folding rate? *Curr. Biol.* 7, R380–R383.
13. Plaxco, K. W. & Baker, D. (1998). Limited internal friction in the rate-limiting step of a two-state protein folding reaction. *Proc. Natl Acad. Sci. USA*, 95, 13591–13596.
14. Kleinert, T., Doster, W., Leyser, H., Petry, W., Schwarz, V. & Settles, M. (1998). Solvent composition and viscosity effects on the kinetics of CO binding to horse myoglobin. *Biochemistry*, 37, 717–733.
15. Jacob, M., Geeves, M., Holtermann, G. & Schmid, F. X. (1999). Diffusional barrier crossing in a two-state protein folding reaction. *Nature Struct. Biol.* 6, 923–926.
16. Ladurner, A. G. & Fersht, A. R. (1999). Upper limit of the time scale for diffusion and chain collapse in chymotrypsin inhibitor 2. *Nature Struct. Biol.* 6, 28–31.
17. Jacob, M. & Schmid, F. X. (1999). Protein folding as a diffusional process. *Biochemistry*, 38, 13773–13779.
18. Bilsel, O. & Matthews, C. R. (2000). Barriers in protein folding reactions. *Adv. Protein Chem.* 53, 153–207.
19. Pabit, S. A., Roder, H. & Hagen, S. J. (2004). Internal friction controls the speed of protein folding from a compact configuration. *Biochemistry*, 43, 12532–12538.
20. Sinha, K. K. & Udgaonkar, J. B. (2005). Dependence of the size of the initially collapsed form during the refolding of barstar on denaturant concentration: evidence for a continuous transition. *J. Mol. Biol.* 353, 704–718.
21. Kramers, H. A. (1940). Brownian motion in a field of force and the diffusion model of chemical reactions. *Physica*, 7, 284–304.
22. Hynes, J. T. (1985). Chemical reaction dynamics in solution. *Annu. Rev. Phys. Chem.* 36, 573–597.
23. Gavish, B. (1986). Molecular dynamics and the transient strain model of enzyme catalysis. In *The Fluctuating Enzyme* (Welch, G. R., ed), pp. 263, Wiley and Sons, New York.
24. Gutfreund, H. (1995). *Kinetics for the Life Sciences*. Cambridge University Press, Cambridge, UK.
25. Hurler, M. R., Michelotti, G. A., Crisanti, M. M. & Matthews, C. R. (1987). Prediction of the tertiary structure of the alpha-subunit of tryptophan synthase. *Proteins: Struct. Funct. Genet.* 2, 54–63.
26. Teschner, W., Rudolph, R. & Garel, J. R. (1987). Intermediates on the folding pathway of octopine dehydrogenase from *Pecten jacobaeus*. *Biochemistry*, 26, 2791–2796.
27. Viguera, A. R. & Serrano, L. (1997). Loop length, intramolecular diffusion and protein folding. *Nature Struct. Biol.* 4, 939–946.
28. Timasheff, S. N. (1993). The control of protein stability and association by weak interactions with water: how do solvents affect these processes? *Rev. Biophys. Biomol. Struct. Annu.* 22, 67–97.
29. Shastry, M. C. & Udgaonkar, J. B. (1995). The folding mechanism of barstar: evidence for multiple pathways and multiple intermediates. *J. Mol. Biol.* 247, 1013–1027.
30. Agashe, V. R., Schmid, F. X. & Udgaonkar, J. B. (1997). Thermodynamics of the complex protein unfolding reaction of barstar. *Biochemistry*, 36, 12288–12295.
31. Zaidi, F. N., Nath, U. & Udgaonkar, J. B. (1997). Multiple intermediates and transition states during protein unfolding. *Nature Struct. Biol.* 4, 1016–1024.
32. Pradeep, L. & Udgaonkar, J. B. (2002). Differential salt-induced stabilization of structure in the initial folding intermediate ensemble of barstar. *J. Mol. Biol.* 324, 331–347.
33. Sridevi, K. & Udgaonkar, J. B. (2003). Surface expansion is independent of and occurs faster than core solvation during the unfolding of barstar. *Biochemistry*, 42, 1551–1563.
34. Pradeep, L. & Udgaonkar, J. B. (2004). Osmolytes induce structure in an early intermediate on the folding pathway of barstar. *J. Biol. Chem.* 279, 40303–40313.
35. Sridevi, K., Lakshmikanth, G. S., Krishnamoorthy, G. & Udgaonkar, J. B. (2004). Increasing stability reduces conformational heterogeneity in a protein folding intermediate ensemble. *J. Mol. Biol.* 337, 699–711.
36. Sato, S., Sayid, C. J. & Raleigh, D. P. (2000). The failure of simple empirical relationships to predict the viscosity of mixed aqueous solutions of guanidine hydrochloride and glucose has important implications for the study of protein folding. *Protein Sci.* 9, 1601–1603.
37. Beece, D., Eisenstein, L., Frauenfelder, H., Good, D., Marden, M. C., Reinisch, L. *et al.* (1980). Solvent viscosity and protein dynamics. *Biochemistry*, 19, 5147–5157.
38. Somogyi, B., Punyiczki, M., Hedstrom, J., Norman, J. A., Prendergast, F. G. & Rosenberg, A. (1994). Coupling between external viscosity and the intramolecular dynamics of ribonuclease T1: a two-phase model for the quenching of protein fluorescence. *Biochim. Biophys. Acta*, 1209, 61–68.
39. Haas, E., Katchalski-Katzir, E. & Steinberg, I. Z. (1978). Brownian motion of the ends of oligopeptide chains in solution as estimated by energy transfer between the chain ends. *Biopolymers*, 17, 11–31.
40. Timasheff, S. N. (1998). Control of protein stability and reactions by weakly interacting cosolvents: the simplicity of the complicated. *Adv. Protein Chem.* 51, 355–432.
41. Record, M. T., Jr, Zhang, W. & Anderson, C. F. (1998). Analysis of effects of salts and uncharged solutes on protein and nucleic acid equilibria and processes: a practical guide to recognizing and interpreting polyelectrolyte effects, Hofmeister effects, and osmotic effects of salts. *Adv. Protein Chem.* 51, 281–353.
42. Anderson, C. F. & Record, M. T., Jr (1993). The salt-dependence of oligoion-polyion binding: a thermodynamic description based on preferential interaction coefficients. *J. Phys. Chem.* 97, 7116–7126.
43. Otting, G., Liepinsh, E. & Wüthrich, K. (1991). Protein hydration in aqueous solution. *Science*, 254, 974–980.
44. Brunne, R. M., Liepinsh, E., Otting, G., Wüthrich, K. & van Gunsteren, W. F. (1993). Hydration of proteins. A comparison of experimental residence times of water molecules solvating the bovine pancreatic trypsin inhibitor with theoretical model calculations. *J. Mol. Biol.* 231, 1040–1048.
45. Svergun, D. I., Richard, S., Koch, M. H., Sayers, Z., Kuprin, S. & Zaccai, G. (1998). Protein hydration in solution: experimental observation by X-ray and neutron scattering. *Proc. Natl Acad. Sci. USA*, 95, 2267–2272.
46. Denisov, V. P., Jonsson, B.-H. & Halle, B. (1999). Hydration of denatured and molten globule proteins. *Nature Struct. Biol.* 6, 253–260.
47. Pal, S. K., Peon, J. & Zewail, A. H. (2002). Ultrafast surface hydration dynamics and expression of protein functionality: alpha-Chymotrypsin. *Proc. Natl Acad. Sci. USA*, 99, 1297–15302.
48. Halle, B. & Davidovic, M. (2003). Biomolecular

- hydration: from water dynamics to hydrodynamics. *Proc. Natl Acad. Sci. USA*, 100, 12135–12140.
49. Kamal, J. K., Zhao, L. & Zewail, A. H. (2004). Ultrafast hydration dynamics in protein unfolding: human serum albumin. *Proc. Natl Acad. Sci. USA*, 101, 13411–13416.
50. Longworth, L. G. (1954). Temperature dependence of diffusion in aqueous solutions. *J. Chem. Phys.* 58, 770–773.
51. Lakshmikanth, G. S. & Krishnamoorthy, G. (1999). Solvent-exposed tryptophans probe the dynamics at protein surfaces. *Biophys. J.* 77, 1100–1106.
52. Gekko, K. (1982). Calorimetric study on thermal denaturation of lysozyme in polyol-water mixtures. *J. Biochem. (Tokyo)*, 91, 1197–1204.
53. Khurana, R. & Udgaonkar, J. B. (1994). Equilibrium unfolding studies of barstar: evidence for an alternative conformation which resembles a molten globule. *Biochemistry*, 33, 106–115.
54. Schellman, J. A. (1987). The thermodynamic stability of proteins. *Annu. Rev. Biophys. Biophys. Chem.* 16, 115–137.
55. Schellman, J. A. (1990). A simple model for solvation in mixed solvents. Applications to the stabilization and destabilization of macromolecular structures. *Biophys. Chem.* 37, 121–140.

Edited by K. Kuwajima

(Received 18 July 2006; received in revised form 26 October 2006; accepted 22 November 2006)
Available online 1 December 2006